

PREPARATION AND OPTICAL PROPERTIES OF SeS THIN FILMS SEMICONDUCTING CHALCOGENIDE GLASSES

M. Abdel Rafea*, A. A. M. Farag^a

Institute of Advanced Technology and New Materials, Mubarak City for Scientific Research and Technology Applications, New Borg El Arab city, Alexandria, Egypt.

^a*Faculty of Education, Ain shams university, Heliopolis, Roxy, Cairo 11757, Egypt*

Se_{1-x}S_x glassy films have been prepared in the thin films form with x in the range 0.0-0.4 and thickness in the range 500-600 nm by thermal vacuum evaporation technique. The amorphous structure of the films was confirmed by XRD measurements. The surface morphology and the thickness of the films were studied by SEM. The optical properties of the films were studied by transmittance method, it was found that the optical constants of the films are sensitive to composition. The refractive index was determined and the data was discussed in the Wemple and DiDomenico model for single effective oscillator. The resultant oscillator energy and strength were then calculated and found to be increased as the composition increases. A blue shift in the absorption edge was observed by increasing the sulfur content and the band gap increases from 1.85 to 2.03 eV as the composition increases from 0.0 to 0.4.

(Received February 14, 2008; accepted February 20, 2008)

Keywords: Chalcogenide glasses, Thermal vacuum evaporation, Optical properties

1. Introduction

Chalcogenide glasses "sulfide, selenide and telluride" in the binary and multi component systems are promising materials for various electronic, optoelectronic, optical memory switching devices, optical recording media and photonic applications. Selenium based chalcogenide glasses have high transparency in the broad middle and far infrared region and have strong non-linear properties. The glassy state Se-S exhibits an electronic conductivity of p-type semiconductor. The addition of S to Se leads to a decrease in the density as well as an increase in the glass transition temperature [1-3]. Substitution of chalcogenide partially by Ge and As increases their thermal stability, while Sb increases their fast phase transformation for optical memory recording media. When Se content increases in the Ge_{0.23}Sb_{0.07}S_{0.70-x}Se_x glass system from 0.0 to 0.7, a red shift of the optical absorption edge occurs. The laser irradiation results in near-surface photo-expansion and glass structure modification as a function of S/Se ratio takes place [4]. In Ge_{30-x}Sb_xS₇₀ glass thin films, the band gap decreases from 2.04 to 1.74 eV as Sb increases from 0 to 30 which was explained by the change of the binding energies of Ge-S and Sb-S. The Wemple & DiDomenico model (WDD) determines the oscillator energy, E_0 , and oscillator strength, E_d , for single effective oscillator using the following formula

$$\frac{1}{n^2 - 1} = \frac{E_0}{E_d} - \frac{(h\nu)^2}{E_0 E_d} \quad (1)$$

Both E_0 and E_d decreases linearly as Sb content increase[5]. Replacing Ge-Sb by As, in the As₃₃S_{67-x}Se_x glass of spin coated films of x = 0 - 67, the increase of Se content decreases the band gap from 2.45 to 1.8 eV. Also a red shift in the absorption edge takes place by annealing the films at T=150 °C for 30 and 60 min [6]. In As_{100-x}S_x glass system, the band gap increases as x decreases. The refractive index is fitted also to the (WDD) dispersion relationship of the single oscillator model [7]. In the As₄₀S_{60-x}Se_x glass system, the glass transition

*Corresponding author: m.abdelrafea@mucsat.sci.eg

temperature decreases from 215 to 114 °C as x increases from 0 to 60, besides large red shift is obtained in absorption curves [8,9]. P-type S_xSe_{100-x} films were deposited on n-Si with $x= 0.25- 7.28$. Good rectifying curves were obtained. The photovoltaic parameters of this type of solar cells were determined with efficiency 4.28 % which decreases as x increases [10]. Doping of the AsS, AsSe and AsSSe glass systems with rare-earth elements shows photoluminescence properties. Both position and line width of the luminescence band are not strongly temperature dependent at lower temperatures but considerable dependence appears at room temperature [11]. The optical properties and the thermal characterization data were measured for Se-S glasses contain additives of PbI_2 , Sb, As and Bi [12]. Replacing S by Te in the SeTeGe glass system reduces the band gap. Also the band gap decreases as annealing temperature increases, which was explained by the crystallization process [13,14]. The annealing temperature dependence of the band gap in $Se_{0.85}Te_{0.15}$ glass films shows a slight increase in E_g from 1.09 to 1.16 eV as annealing temperature increases up to $T_g= 353$ K. This behavior was explained on the basis of the Mott - Davis model for the density of states in amorphous solids. When annealing temperature increases from 353 to 385K, E_g decreases gradually to a value of 0.67 eV which was suggested that the amorphous–crystalline phase transformation is responsible for the decrement of the band gap [15].

The aim of this work is to study the optical properties of $Se_{1-x}S_x$ glass system in the composition range 0.0-0.4, which has not been studied optically before.

2. Experimental

Selenium and sulfur elements of purities “5N Acros-Organics”, were used to prepare $Se_{1-x}S_x$ system in the composition range $x=0-0.4$. Fine powder of Se and S were mixed and mechanically alloyed in a hardened agate in order to obtain homogeneously well mixed powder "this method was used in ref [16]". Pellets of diameters 10mm and thickness 2 mm were prepared by hydraulic press at 8 kN/cm² under vacuum. 200 mg of the pressed material was evaporated in a Mo boat under high vacuum of $0.6-2 \times 10^{-5}$ Torr using a standard Edwards A306 Auto coating unit with conventional rotary and turbo molecular pumps.

Glass substrate was cleaned several times ultrasonic cleaner using detergent, Double distilled water and ethyl alcohol final washing, furthermore a glow discharge cleaner in the vacuum system was then clean the substrates before evaporation. The glass substrates were fixed in the rotating substrate work holder with adjusted and fixed rotating speed that produces films with high homogeneity and constant thickness. The substrate temperature was at room temperature during evaporation and evaporation rate was in the range 30-40 Å/sec .

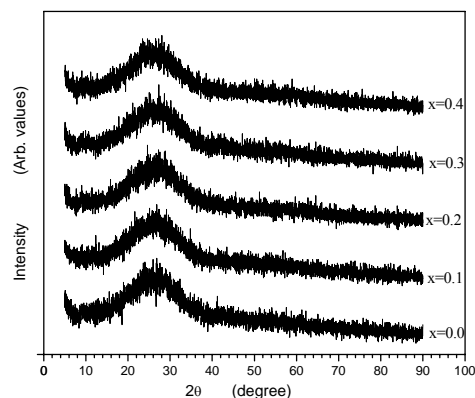


Fig. 1. XRD chart for $Se_{1-x}S_x$ with $0.0 \leq x \leq 0.4$.

The structure of the deposited films was studied using XRD and SEM. A Shimadzu XRD 7000 maxima powder diffraction was used at the conditions "tube voltage 30 KV, current 30 mA and wavelength $CuK\alpha_1$, $\lambda=1.5406$ Å. The scan range $2\theta=5-90^\circ$ and scan speed $1^\circ/\text{min}$. SEM of type Jeol-JSM-636 OLA was used to

study the surface morphology of the deposited films. The cross sectional imaging of the film and the substrate also determine the films thickness at different points of the broken edge. The optical transmittance of the films was measured using SPECTRO UV-VIS DOUBLE BEAM UVD2950 PC SCANNING LABOMED spectrophotometer and a reference glass substrate was used in the spectral range 190-1100 nm.

3. Results and discussion

X-ray diffraction measurement confirms the amorphous structure of the films. No characteristic diffracted peaks of Se, S or SeS system were resolved. Only the amorphous behavior in the chart is observed as shown in Fig.(1). A representative picture of scanning electron micrograph for film with $x=0.2$ shows that there is no characteristic features observed on the surface morphology of the films i.e no grains appear. Fig.(2.a) shows the cross sectional image of SEM. The picture resolves the film “white” and the substrate “dark below”. The cross section view shows that the film consists of two parallel surfaces, the difference between them is the thickness. The value of the film thickness was averaged for several positions and pictures for each composition and presented in table (1).

Table 1. The measured thickness by the cross section image of SEM.

x	0.0	0.1	0.2	0.3	0.4
d	615 ± 18	540 ± 23	593 ± 27	583 ± 19	492 ± 19

Table 2. Calculated Optical constants of the $Se_{1-x}S_x$ with $0.0 \leq x \leq 0.4$.

x	n ($\lambda > 700nm$)	k ($\lambda > 700nm$)	E_g eV	E_o eV	E_d eV
0.0	2.32 ± 0.06	0.028 ± 0.001	1.85	10.21	3.06
0.1	2.17 ± 0.01	0.018 ± 0.001	1.92	14.24	4.37
0.2	2.15 ± 0.01	0.022 ± 0.002	1.96	17.03	5.19
0.3	1.98 ± 0.02	0.034 ± 0.002	2.05	7.10	3.16
0.4	1.92 ± 0.01	0.031 ± 0.002	2.03	12.59	4.93

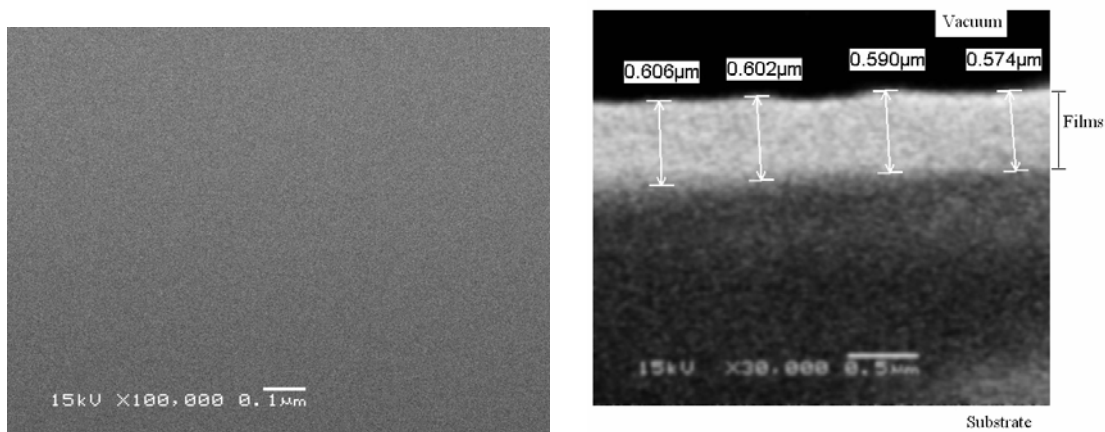


Fig. 2. Representative pictures SEM micrograph of $Se_{0.8}S_{0.2}$ film. (a). The surface image, (b). The cross section image.

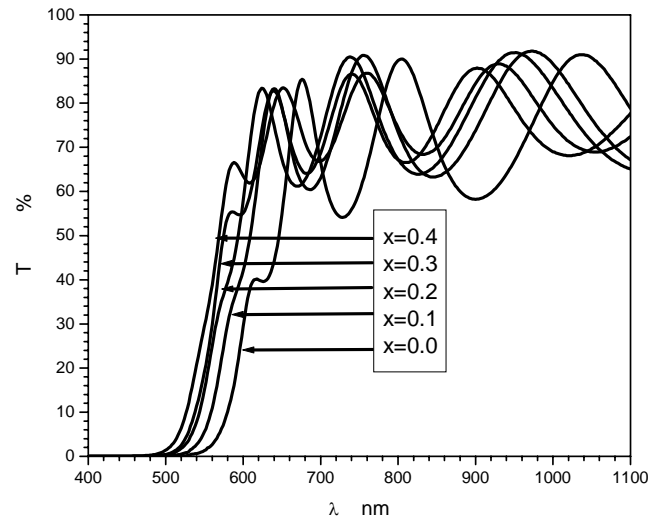


Fig. 3. Optical transmittance of $Se_{1-x}S_x$ films with $0.0 \leq x \leq 0.4$.

The optical transmittance curves of the films shows high transmittance about 80 % below the fundamental absorption edge as shown in Fig.(3). The absorption edge is blue shifted as x increases, which explains the color change of the films. Maxima and minima appear in the transmittance curve due to interference; this phenomenon takes place only in high quality films with good surface properties. Thirdly, the absorption edge shifted as x increases. The envelope method was used to determine the optical constants and study the optical properties of the films [17]. The refractive indices and the extinction coefficients were calculated and plotted against the wavelength as shown in Fig.(4) and Fig.(5). Both n and k increases slowly with decreasing the wavelength. A considerable sharp increase near the absorption edge was observed due to high absorption process. The refractive index and the extinction coefficient in the transparent region ($\lambda > 700$ nm) decrease with increasing x as shown in table (2). The (WDD) model was applied to analyze the refractive indices taking in considerations the lower energy part. The data of very low photon energy were excluded due to constant refractive index (optical refractive index), the values near the absorption edge are also excluded. Fig.(6) shows the plot of $(n^2 - 1)^{-1}$ vs $(h\nu)^2$ linear dependence is obtained. The values of E_o and E_d are directly determined from the slope $(E_o E_d)^{-1}$ and the intersect (E_o/E_d) . The slopes at higher compositions are either very high at 0.3 or very low at 0.4 in compared behavior or the other compositions. The first three compositions are shown in table (2), both of the oscillator energy, E_o and oscillator strength, E_d , increases with increasing the sulfur content. The increase of the values of E_d and E_o based on the Wemple equation, are related to the change of the binding energy between Se-S and the number of nearest S toms to the Se (coordination number) that are changed by increasing the composition which was discussed similarly for another chalcogenide systems [5,18].

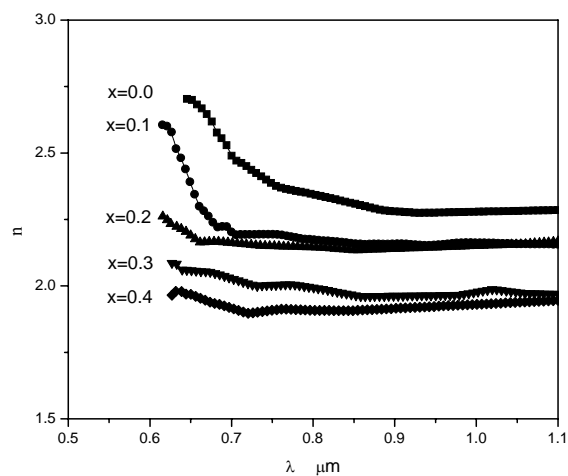


Fig.4. n - λ relationship for $Se_{1-x}S_x$ films with $0.0 \leq x \leq 0.4$.

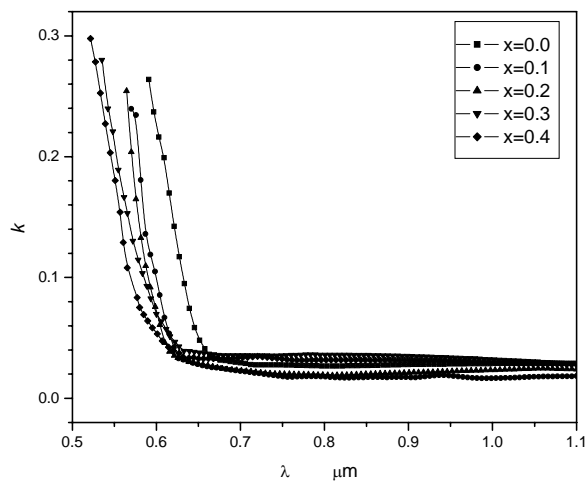


Fig.5. k - λ relationship for $Se_{1-x}S_x$ films with $0.0 \leq x \leq 0.4$.

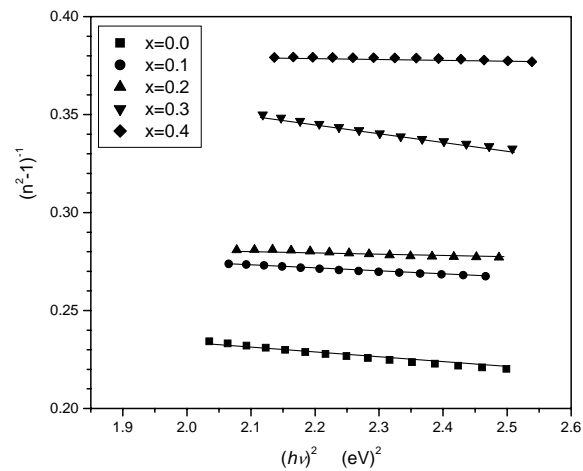


Fig.6. (WDD) model applied for $Se_{1-x}S_x$ films with $0.0 \leq x \leq 0.4$.

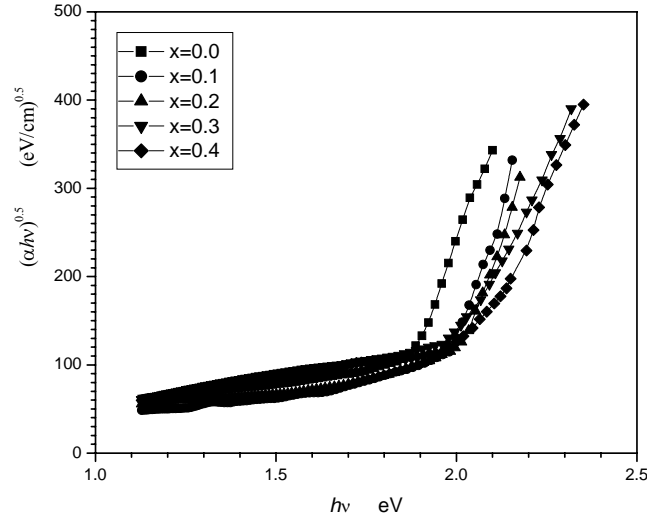


Fig.7. $(\alpha h\nu)^{0.5}$ vs $h\nu$ for $Se_{1-x}S_x$ films with $0.0 \leq x \leq 0.4$.

The absorption coefficient, α , was calculated as, $\alpha = \frac{4.\pi.k}{\lambda}$. In non-crystalline systems the non-direct transitions are most likely to occur due to the absence of translation Symmetry. The present results were found to obey the allowed non-direct transition [19]. In the fundamental, the intercept of the plot $(\alpha h\nu)^{0.5}$ vs $h\nu$ with the $h\nu$ axis determines E_g as shown in Fig.(7). The calculated E_g is shown in table (2). As x increases the band gap increases which explain the red yellowish change from dark red of the films as the sulfur content increase. This also agree with *Nadeem Musahwar* [3] *et al* in measurements of dielectric properties and the temperature dependence of the a.c. and dc conductivities, they suggested that, increasing sulfur in Se-S glasses reduces defects which may increase the band gap.

4. Conclusions

We can conclude from our study of Se-S semiconducting glasses that:-

- High quality $Se_{1-x}S_x$ amorphous films with $0.0 \leq x \leq 0.4$. were deposited from pressed powder which was prepared by mechanical alloy method.
- The refractive index and extinction coefficient in the transparent region of the spectrum were found to be decreased as sulfur content increases.
- The refractive index and their behavior with the incident photon energy was discussed in the (WDD) model of the single effective oscillator, the oscillator energy and strength were also determined and discussed was the change of the composition.
- The band gap was determined for films, it was found to be in the range 1.85-2.03 eV, and increases as the composition increase.

Acknowledgment

This work was carried out through the support from the Mubarak City for Scientific Research and Technology Applications (MUCSAT), projects program of the Institute of Advanced Technologies and New materials.

References

- [1] A.M.A. EL-Barry Physica **B 396**, 49 (2007).
- [2] D. Lezal, J. Pedikova, J. Javadi, J. Optoelectron. Adv. Mater. **6**(1), 133 (2004).
- [3] Nadeem Musahwar, M.A. Majeed Khan, M. Husain, M. Zulfequar Physica B **396**, 81 (2007).
- [4] L. Petit, N. Carlie, T. Anderson, M. Couzi, J. Choi, M. Richardson, K.C. Richardson, Optical Materials **29**, 1075 (2007).
- [5] El-Sayed M. Farg, Optics & Laser Technology, Received 13 April 2004; revised form 21 October 2004; accepted 8 November 2004.
- [6] T. Kohoutek, T. Wagner, Mir. Vlcek, Mil. Vlcek, M. Frumar, Journal of Non-Crystalline Solids **352**, 1563 (2006).
- [7] E.R. Shaaban, N. El-Kabnay, A.M. Abou-sehly, N. Afify, Physica B **381**, 24 (2006).
- [8] T. Cardinal, K. A. Richardson, H. Shim, A. Schulte, R. Beatty, K. Le Foulgoc, C. Meneghini, J. F. Viens, A. Villeneuve, J. Non-Crystalline Solids **256&257**, 353 (1999).
- [9] K. Petkov, P. J. S. Ewen, J. Non-Crystalline Solids **249**, 150 (1999).
- [10] M.M. El-Nahass, H.E.A. El-Sayed, A.M.A. El-Barry, Solid-State Electronics **50**, 355 (2006).
- [11] D. Lezal, J. Pedlikov, J. Zavadil, P. Kostka, M. Poulain, J. Non-Crystalline Solids **326-327**, 47 (2003).
- [12] J. Troles, F. Smektala, Y. Jestin, L. Begoin, S. Danto, M. Guignard, J. Non-Crystalline Solids **352**, 248 (2006).
- [13] A. El-Korashy, A. Bakry, M. A. Abdel-Rahim, M. Abd El-Sattar, Physica B **391**, 266 (2007).
- [14] E.R. Shaaban, M. Abdel-Rahman, El Sayed Yousef, M.T. Dessouky, Thin Solid Films **515**, 3810 (2007).
- [15] A.S. Soltan, M. Abu EL-Oyoun, A.A. Abu-Sehly, A.Y. Abdel-Latief, Materials Chemistry and Physics **82**, 101 (2003).
- [16] S.M. El-Sayed, Vacuum **65**, 177 (2002).
- [17] H. Demiryont, James R, Kent Geib, Applied Optics, **24**(15), 490 (1985).
- [18] A. M. Salem, S.Y. Marzouk, S.H. Moustafa, M.S. Selim, Nuclear Instruments and Methods in Physics Research B **262**, 225 (2007).
- [19] S. A. Fayek, S. M. El Sayed, A. Mehana, A. M. Hamza, J of Materials Science **36**, 2061 (2001).